Cytotechnology **24:** 201–212, 1997.
© 1997 *Kluwer Academic Publishers. Printed in the Netherlands.*

Development of resting membrane potentials in differentiating murine neuroblastoma cells (N1E-115) evaluated by flow cytometry

William S. Kisaalita[1] & John M. Bowen[2]
[1] *Biological and Agricultural Engineering Department, Driftmier Engineering Center;* [2] *Department of Physiology and Pharmacology, College of Veterinary Medicine, University of Georgia, Athens, Georgia 30602*

Received 29 March 1996; accepted in final form 2 September 1996

Key words: electrophysiological differentiation, flow cytometry, membrane potential, N1E-115 neuroblastoma cells

Abstract

With the aid of a voltage-sensitive oxonol dye, flow cytometry was used to measure relative changes in resting membrane potential (V_m) and forward angle light scatter (FALS) profiles of a differentiating/differentiated murine neuroblastoma cell line (N1E-115). Electrophysiological differentiation was characterized by V_m establishment. The (V_m)-time profile was found to be seed cell concentration-dependent for cell densities of less than 2×10^4 cells/cm^2. At higher initial cell densities, under differentiating culture conditions, V_m development commenced on day 2 and reached a steady- state on day 12. The relative distribution of differentiated cells between low and high FALS has been proposed as a potential culture electrophysiological differentiation state index. These experiments offer a general methodology to characterize cultured excitable cells of nervous system origin, with respect to electrophysiological differentiation. This information is valuable in studies employing neuroblastoma cells as *in vitro* screening models for safety/hazard evaluation and/or risk assessment of therapeutical and industrial chemicals under development.

Introduction

The complexity and diversity of the nervous system has precluded the rapid development of *in vitro* alternatives for neurotoxicity testing (Williams et al., 1994). However, recent commercial pressures and regulatory requirements have heightened interest in this area. For example, the EPA has stated that neurotoxicology should have high priority and that the development of methods for the identification of neurotoxic risk must be intensified in order to improve human risk assessment (EPA, 1991). To date, proposed guidelines for neurotoxicity testing involve only animal-based models and are therefore expensive and time consuming. Besides, some biotechnological compounds with therapeutical value (e.g. antibodies and peptides) are human specific compounds animals may not respond to. As such the EPA, as well as other regulatory agencies, are examining ways to utilize *in vitro* testing (using cells of human origin) in human risk assessment (Veronesi, 1992).

Due to the low regenerative capacity of the nervous system, Walum et al. (1993) has suggested that cellular tests included in primary screens should be based on determination of cellular dynamic physiological parameters, such as alteration in membrane function, rather than measurement of a single biochemical reaction. Our interest in this regard is to use neuroblastoma cells in the development of *in vitro* neurotoxicity test with alteration in resting membrane potential (V_m) and/or electrical excitability as an endpoint. This effort is based on the assumption that neurotoxic effects in cellular models (nervous system cells) are important for toxicological pre-screening, identification of potential neurotoxic compounds and for elucidation of the mode of action.

Neuroblastomata are precursors of sympathetic ganglia (a component of the peripheral autonomic nervous system) derived from malignant tumors originating from neural crest cells (Ishikawa, 1977). The neural crest is the thickened ectoderm around the edge of the embryonic neural plate. As the neural plate closes to

form the neural tube, the neural crest cells are released from their position in the neural fold (Tosney, 1982). Although the neural fold consist of two additional cell types (the internally positioned neural tube cells and the epidermis of the skin), only the cells which migrate are called neural crest cells. The mechanism of release from of the neural crest cells is still unknown. N1E-115 is a clonal line derived from a spontaneously arising murine neurablstoma C1300 (Augusti-Tocco and Sato, 1969; Amano et al., 1972).

N1E-115 cells were selected for our long-term studies for several reasons. First, Mummery et al. (1984) successfully used N1E-115 cells in an assay for teratogenic compounds based on the ability of the agents to interfere with normal growth and morphological differentiation. Morphological differentiation of N1E-115 cells and other neuronal cells is defined simply as the appearance of one (or more) neuritic processes longer than the somatic diameter (Mummery et al., 1984). Neuronal electrophysiological differentiation is characterized by the ability of the cell to generate repetitive discharges either spontaneously or in response to stimulation (Tuttle and Richelson, 1975; Moolenaar and Spector, 1977; Quandt et al., 1984). This is achieved at elevated V_m and reflects the development of functional Na^+ and K^+ channels that underlie the fast action potential and of functional Ca^{2+} and Ca^{2+}-activated K^+ channels that underlie slow repetitive discharges (Fishman and Spector, 1981; Spector, 1981). Since a temporal separation of morphological and electrophysiological differentiation of N1E-115 cells has been reported (Cosgove and Cobbett, 1991), the extension of Mummery and co-workers' previous results beyond morphological differentiation is justifiable. Secondly, in a previous study by Walum et al. (1987) with three neuroblastomas (41A3, N-18, and N1E-115), a glioma $\times$ neuroblastoma hybrid (NG108CC15), two gliomas (138MG and C6), and two fibroblasts (RFL and RMC), N1E-115 and NG108CC15 showed the highest sensitivity to the neurotoxic compound, acrylamide. Walum et al. (1987) attributed the high sensitivity to the fact that both N1E-115 and NG108CC15 cells express a number of neuronal properties and were the most morphologically differentiated of all the cell lines tested. Thirdly, differentiated N1E-115 cells are considered excellent neuronal models. A number of investigations have indicated that the transition of N1E-115 cultures from the rapidly dividing to confluent state results in the appearance of several morphological, biochemical, and electrophysiological indices of *in vivo* differentiation (Nelson et al., 1969; Amano et al., 1972; Gilbert et al., 1982).

Changes in membrane electrical properties of N1E-115 have been previously studied by intracellular or whole-cell patch clamp recording techniques that rely on the use of glass microelectrodes (Kimhi et al., 1976; Kato and Narahashi, 1982; Cosgrove and Gobbett, 1991; Zwart et al., 1994). One of the main drawbacks with these techniques is the number of cells analyzed, usually limited to 20 cells per culture. Use of voltage-dependent fluorescent probes is a more desirable alternative because many thousands of cells can be analyzed over a short period by flow cytometry (Dwyer and Cuchens, 1987; Krieger et al., 1991). These indicators are a heterogeneous group of substances whose fluorescence varies with the transmembrane potential. Flow cytometry also permits the simultaneous detection of light scatter properties which can be very useful in identifying and separating groups of cells with similar physiological attributes (Givan, 1993). This capability is very important to developing *in vitro* systems based on neutral crest cells, since the neural crest is a pluripotent population of cells that differentiate into a large variety of derivatives including neurons and glial cells of the peripheral nervous system, endocrine cells, melanocytes and the so-called mesectoderm (Couly et al., 1993).

The objective of this study was to use a voltage-sensitive oxonol dye in conjunction with flow cytometry to examine the electrophysiological differentiation of N1E-115 cells [with respect to the development of the resting membrane potential (V_m)] over a period in which these cells have previously been shown to mature into electrically excitable cells (Kimhi et al., 1976; Spector, 1981). Our investigations addressed three related questions: (1) What is the relationship between light scattering properties of N1E-115 cells and electrophysiological differentiation?; (2) When do differentiating N1E-115 cells mature and exhibit steady and maximal V_m?; and (3) What is the effect of initial cell density on the V_m-development profile?

Materials and methods

Cell line and cell culture

N1E-115 cells of passage 12 were obtained from Dr. M. Nirenberg, National Institute of Health (Bethesda, MD). Previously published protocols for N1E-115 cell culture (Kimhi et al., 1976; Miyake and Kurihara,

1983) were followed. Briefly, N1E-115 cells were routinely cultured at 37 °C in air plus 10% CO_2 and at 90% relative humidity. Growth medium was composed of DMEM containing 0.37% $NaHCO_3$ (w/v) and supplemented with 13% FBS, 50 units ml^{-1} penicillin, 50 $\mu g\ ml^{-1}$ streptomycin, and 2 mM glutamine. Cultures were monodispersed gently by flushing the confluent cells from the base of a 75-cm^2 T-flask (Costar, Cambridge, MA) by a stream of medium ejected from a Pasteur pipet. The suspension was centrifuged (50 × g; 10 min) and the pellet resuspended in 25-cm^2 T-flasks (Costar, Cambridge, MA) with fresh growth medium at 2.0×10^6 viable cells (able to exclude trypan blue) per flask, unless otherwise stated. Flasks (in triplicate) were incubated overnight (24 hours) to allow cells to settle and adhere to the base of the flask. Cells were then exposed to the differentiating medium (same as the growth medium except serum was reduced to 0.5%). Previously, N1E-115 cells were shown to be electrically active when differentiated with dibutyryl cyclic AMP (Chaizonitis and Green, 1974; Kato and Narahashi, 1982), 1–2% dimethyl sulfoxide (Kimhi et al., 1976), reduced serum levels in the growth medium (Seeds et al., 1970) and aminopterin selection (Tuttle and Richelson, 1975). In this study, the choice of N1E-115 cell differentiation by serum reduction from 13% (control) to 0.5% was justified in a separate study (Kisaalita and Bowen, 1996). The differentiating medium was changed every 3 to 4 days. Relative resting membrane potentials were determined by flow cytometry at time intervals of approximately 3 days, after low-serum exposure.

Potential-sensitive probe

The negatively charged oxonol dyes undergo V_m-dependent distribution between the cytoplasm and the extracellular medium and are generally less toxic to cells than the carbocyanines (Kohen and Hirscherg, 1989). The anionic oxonol dye, bis-(1,3-dibutylbarbituric acid)trimethine oxonol ($DiBAC_4[3]$), was chosen for these experiments since it can reliably indicate V_m without major contributions from the mitochondrial potential, making it superior to carbocyanines for flow cytometry applications (Wilson and Chused, 1985). Cellular loading with oxonol is a function of V_m. As cell depolarization occurs, dye loading increases, causing an increase in fluorescence intensity (Brashford et al., 1985). Therefore, low intensity reflects high V_m and vice versa. The oxonol used in this study has been reported to exhibit the highest voltage sensitivity of all oxonols (Bräuner and Hülser, 1984).

Resting membrane potential determination

Cells were monodispersed, centrifuged (500 × g; 10 min), resuspended in a saline solution and counted with a hemocytometer. The saline solution contained (in mM): 140 NaCl, 5 KCl, 1 MgCl, 1.8 $CaCl_2$, 10 HEPES, 10 D-glucose, pH 7.3. Cells were washed (500 × g, 10 min), resuspended at 0.5×10^6 cells ml^{-1} and incubated with 0.4 μM $DiBAC_4[3]$ and propidium iodide (20 $\mu g\ ml^{-1}$) dyes for 30 min at 37 °C. Flow cytometry analysis of the cell suspension was performed on the University of Georgia (UGA) Research Services' Coulter EPICS 753 (Hialeah, FL) dual-beam instrument. Forward-angle light scatter (FALS), side-light scatter (SSC), oxonol and propidium iodide signals/emissions were obtained in response to argon-ion laser excitation (488 nM) at 200 mW power output (Coherent, Palo Alto, CA). Oxonol emissions were determined by PMT_1 after passage through a 525 nM band-pass filter. Propidium iodide (PI) emissions were determined by PMT_2 after passage through a 610 nM long-pass filter. SSC was determined by PMT_4. FALS signals were linearly amplified with a gain of 2. Unless otherwise stated, 50,000 events were counted at an approximate rate of 200 events per second. Since subcellular debris has low FALS, this parameter was used to gate out these particles. FALS, SSC, and oxonol fluorescence analyses were restricted to events that were PI-negative, since dead or dying cells are stained by PI. In order ro compare results for experiments conducted at different times, polystyrene fluorospheres (Coulter Corporation, Hialeach, FL) were used to set the PMT_1 (oxonol signal) and PMT_4 (SCC signal) at channel numbers of 35 ± 1 and 100 ± 2, respectively, before each experiment.

Viable cell size determination

Viable cells were determined by trypan blue staining. Aliquots (0.1 ml) of monodispersed cells were diluted 1:1 with 0.4% trypan blue (Sigma Chemical Co., St Louis, MO). An aliquot of the mixture was transferred to a hemocytometer and viewed under a Nikon inverted photomicroscope (IMT2) at a magnification of 200×. Viable cells were identified as unstained and non-viable cells stained blue-purple. Viable cell sizes were determined as previously described (Kisaalita et al., 1996). Briefly, an Olympus QUE-3 color image

system was used to acquire enough images to include at least 100 non-stained (viable) cells. A conversion utility (Scott Data Inc., Tonka Bay MN) was used to convert QUE to TIFF files. Cell cross-section areas were extracted from TIFF images with a user defined macro in OPTIMUS image analysis software (Optimas, Edmond, WA).

Results and discussion

Light scatter profiles

A plot of FALS versus SSC revealed two cell populations (high- and low-FALS, Fig. 1A). According to Givan (1993), FALS is light of the same wavelength as the illuminating laser beam that is refracted (or otherwise deflected) as it passes through the cell so as to diverge from the original direction of the laser beam by approximately 0.5 °. FALS is therefore a function of refractive index as well as the cell cross-sectional area. SSC is also light of the same wavelength as the illuminating laser beam that bounces off cells in the orthogonal direction to the laser. The intensity of SSC is related to the roughness (sometimes referred to as irregularity or granularity) and internal components of the cell. The relationship between FALS and PI fluorescence was utilized to clearly separate or 'gate' viable cells (PI-negative) and dead/dying cells (PI-positive) as shown in Fig. 1B. Figures 1C and 1D show the fluorescence histograms for the PI-negative and PI-positive cells as defined in Fig. 1B. As expected, the majority of PI-positive cells exhibited no oxonol fluorescence and therefore showed up in the lowest channel (10^0). The rest of the PI-positive cells that exhibited oxonol fluorescence were considered to be in the process of dying, since both dead and dying cells take up PI.

Figure 2 shows the effect of differentiating culture age on cell distribution between the high- and low-FALS groups. Using the low- and high-FALS gates defined in Fig. 1A, control cultures in the low-FALS group increased from 7.6% at day 2 to 27.9% at day 21 in comparison to differentiating/differentiated low-FALS cultures that increased from 21% to 87.4%. To ascertain if there was any contribution to FALS change from cell size differences, cell size (cross-section area) distribution for control and differentiated cultures at day 12 were compared. Figure 3 shows the cell cross-section area distribution functions. A Mann-Whitney U test (Hogg and Craig, 1995) that uses ranks of individual data points was used to test the null hypothesis (the two cell populations have identical size distributions) and the alternative hypothesis (the two populations are not identically distributed). The null hypothesis was rejected (P=0.0001) and the alternative accepted. This is consistent with the observed shift in the differentiated cell size distribution to the left suggesting that on the average, the differentiated cells were smaller than the control cells. This finding is at odds with previous observations (Peacock et al., 1973; Tuttle and Richelson, 1975), where cell size enlargements were reported for several C1300 clones including N1E-115. This discrepancy has been attributed to differences in techniques for cell size determination. In this study, cells were monodispersed and observed under conditions close to free suspension. In the previous studies, cells were observed in their spread conformation while attached to plates. It is very well known that growth and differentiation of many cell lines follow a two step process. Firstly, cells interact with surfaces by attaching while maintaining the round shape they posses in suspension. Secondly, attachment is followed by a type of conformation change (spreading), in which the cells increase their area in contact with the surface. Spreading is considered essential for growth and differentiation (Ramsden et al., 1993). Possibly, cell size increases reported by Peacock et al. (1973) and Tuttle and Richelson (1995) were due to cell spreading. Such cell spreading has been observed in our laboratory (Kisaalita et al., 1996). Although a reduction in cell size (e.g., from 22 to 19 μm in diameter for the most common cells sizes) was observed for differentiated cells, it was concluded that this reduction could not have contributed significantly to changes in FALS, since a large overlap in the control and differentiated cell size distributions was observed (Fig. 3). A similar conclusion was reached in a separate paper, by comparing experiments with identically distributed control and differentiating cell-sizes, yet exhibiting non-identical FALS profiles (Kisaalita et al., 1996).

The most widely examined markers, for identification of cell types, are generally those appearing when terminal differential has accurred. For example, astrocytes and neurons can be characterized by the expression of glial fibrillary acidic protein (GFAP) and neurofilaments (NF), respectively, with monoclonal antibodies against GFAP and NF (Rouget et al., 1992). The relationship between the ratio of cells in the high- and low-FALS regions and differentiating/differentiated culture age described above has potential as an index of differentiation/differentiated state, applicable before and after terminal differentia-

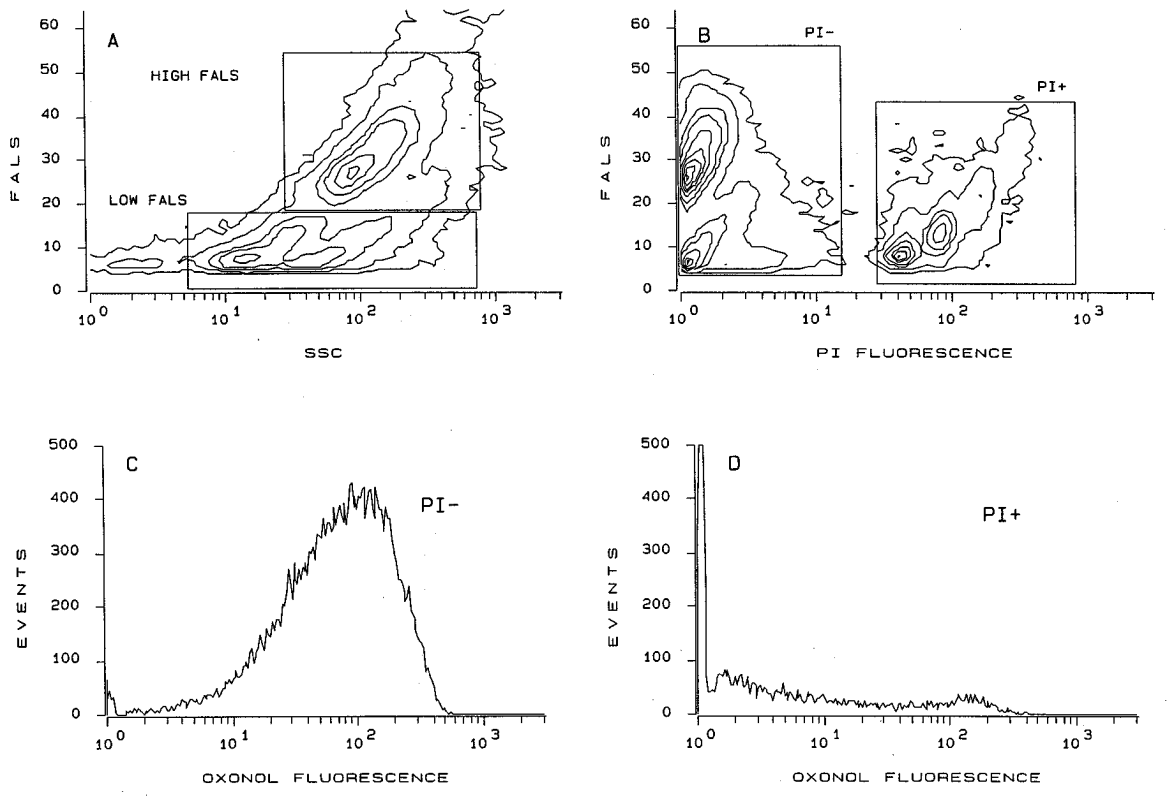

Figure 1. An example, illustrating gating to exclude the dead or dying cells from oxonol fluorescence analysis. Contours in A and B represent 1, 10, 50 and 100 event intervals thereafter. C and D are oxonol fluorescence signals from live and dead/dying cells, respectively.

tion. Studies are underway in our laboratory to extend these findings to other neuroblastoma cells and neuronal primary cultures.

Resting membrane potential development

A qualitative comparison of oxonol fluorescence signals on day 21 for control and differentiated cells is shown in Fig. 4. Shift of the histogram to the left (from channel 200 for control cells to channel 28 for differentiated cells) is indicative of increase in V_m. A plot of the mode channel number against differentiation/differentiated culture age in Fig. 5 revealed three regions of the N1E-115 cells differentiation profile, i.e., 0–7, 7–12, and over 12 days, representing low V_m, rapid V_m rise and steady V_m respectively. To make sure that the shift of histograms to the left as shown in Fig. 4 were due to V_m development and not some other differentiation effect, the external potassium concentration $[K^+]_0$ of a few cell samples was changed before flow cytometry analysis. The V_m at which K^+ ions are in equilibrium (K^+-Nernst potential) across the cell membrane can be calculated from the Nenst equation:

$$V_k = (RT/ZF)\ \ln([K^+]_0/[K^+]_I$$

where V_k is the value of K^+-Nernst potential, R is the gas constant, T the temperature in degrees Kelvin, Z the valence of K^+, F the Faraday constant in coulombs/mole, and $[K^+]_0$ and $[K^+]_I$ the extra- and intra-cellular K^+ concentrations. In nerve cells, the observed V_m matches the calculated V_k at relatively high extracellular K^+ (> 5 mM) (Orkand, 1977). As shown in Fig. 6, increasing $[K]_0$ resulted in the anticipated reduction in V_m, illustrated by the oxonol fluorescence histogram's shift to the right. Differences in the shape of the curves probably suggest that all cells did not respond to $[K^+]_0$ increases in a uniform manner. Although the exact Vm values were not determined by this flow cytometric technique, the results are useful in that the measurements are conducted on a large population of cells, which provides a more accurate indication of the V_m distribution with in the culture.

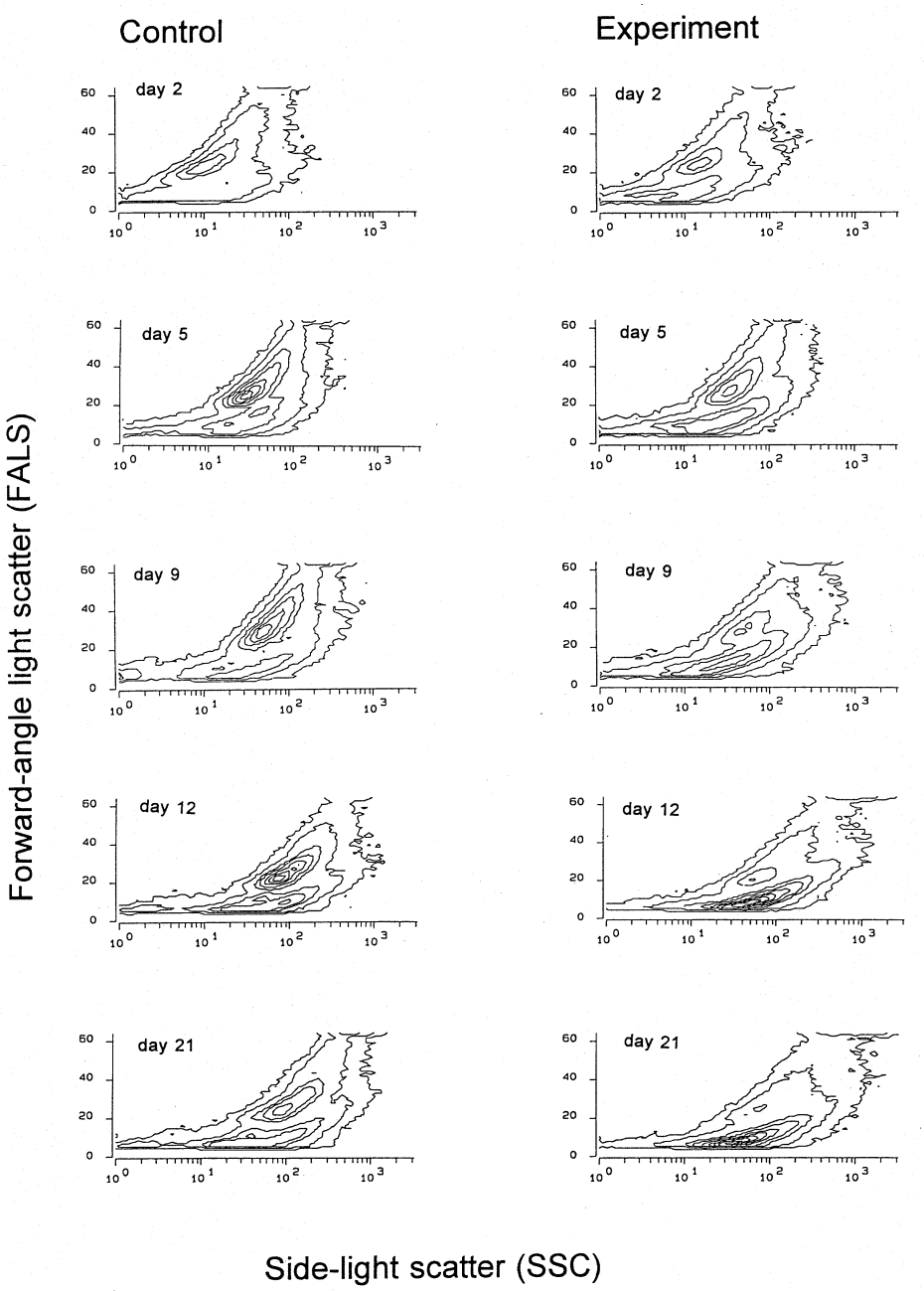

Figure 2. Relation between forward angle light scatter and N1E-115 differentiated and/or differentiating culture age. First, second, third and fourth contours represent 1, 10, 50 and 100 events respectively. Contours greater than 4 represent 100-event increments.

The finding of a period of rapid rise in V_m at approximately 7 to 9 days in this study is consistent with previous results, obtained by intracellular and patch clamp recording techniques. For example, Kimhi et al. (1976) exposed N1E-115 cells to 1, 2 and 4% DMSO. These cells exhibited rise in V_m which reached a maximum after 7–8 days of incubation. In another study, V_m of cells differentiated with N^6,2'-O-dibutyryladenosine 3':5'-cyclic monophosphate reached a plateau value around –50 mV between days 7–8 (Santone et al.,

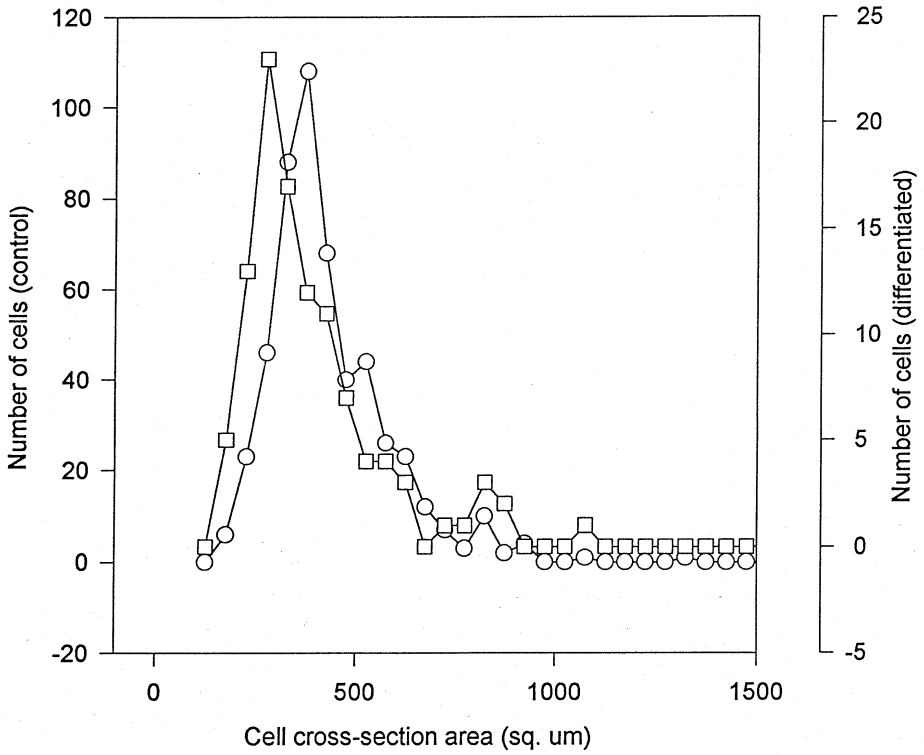

Figure 3. N1E-115 cell size distribution: (○) control culture, (□) differentiated culture (12 days after exposure to the differentiating medium.)

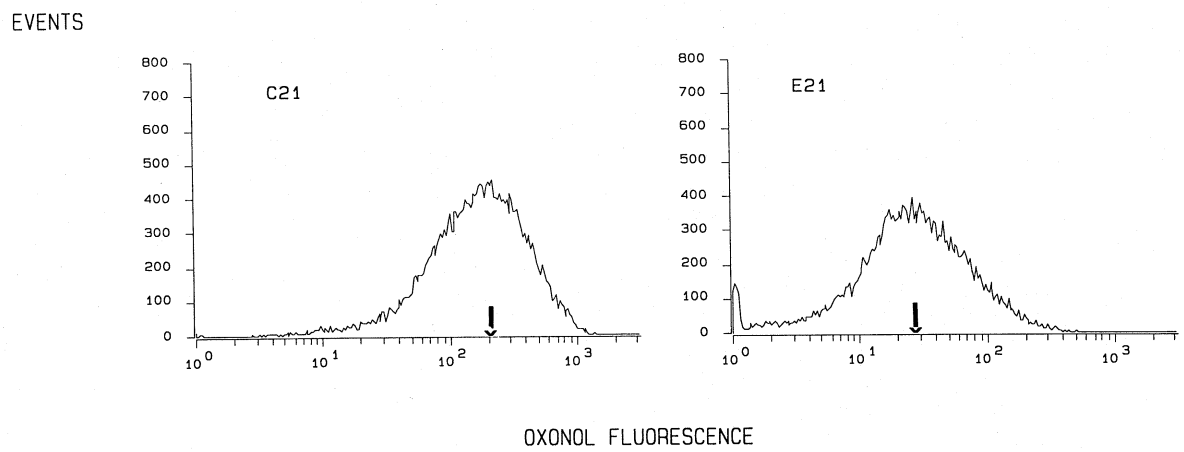

Figure 4. Comparison of control (C21) and differentiating (E21) culture oxonol fluorescence signals after 21 days of incubation with the differentiating medium. Arrows indicate the mode channel numbers of approximately 200 and 28 for control and differentiated cells, respectively.

1986). In a more recent study, Cosgrove and Cobbett (1991) performed electrophysiological recordings from N1E-115 cells maintained in serum-free medium for 2, 4, 8 and 13 days after plating. After 4 days, depolarizing current could elicit a slightly larger depolarization, however, multiple action potentials generated by such current injections were possible only at 8 or 13 days. Also, Baumgold and Spector (1987) showed that

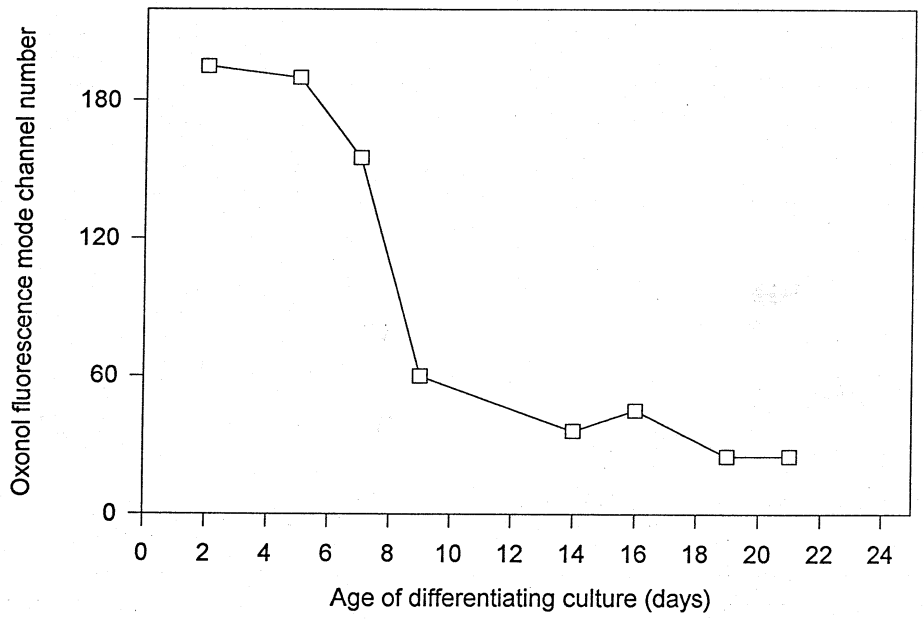

Figure 5. Resting membrane potential development profile of N1E-15 cells based on shift in oxonol fluorescence mode channel number.

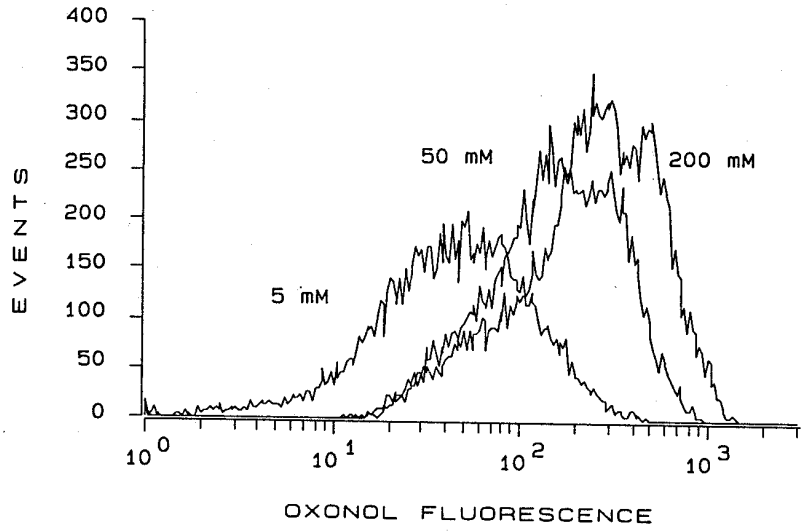

Figure 6. Representative relation between the external K^+ concentration and oxonol fluorescence distribution in N1E-115 cells.

N1E-115 neuroblastoma cells at all stages of growth and differentiation have Na^+ channels and induction of differentiation triggers a significant increase in Na^+ channel density, well after the cells assume the morphologically differentiated state (6-9 days).

Effect of initial cell density

Figure 7 shows fluorescence mode channel number for 15-day old cultures as a function of initial cell concentration. As shown, initial cell density had no effect above 2×10^4 cells cm^{-2}. At lower values, V_m development was slower. Although a temporal separation of morphological and electrophysiological differ-

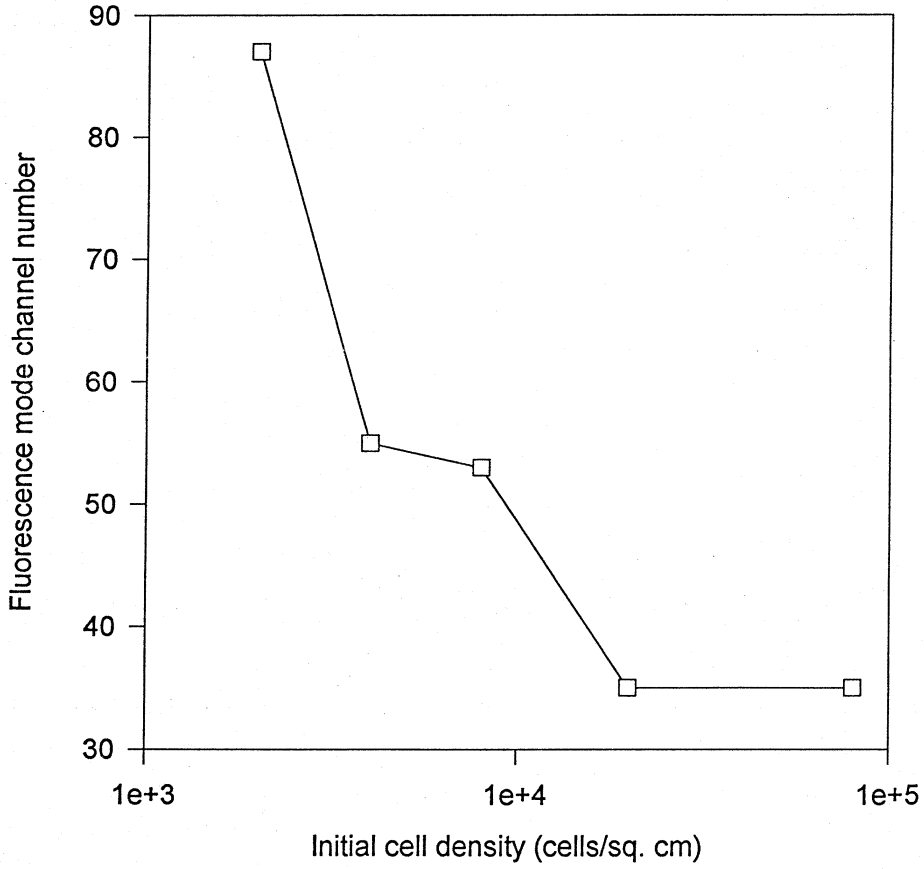

Figure 7. Relation between resting membrane potential development and initial N1E-115 cell density after 15 days of incubation with the differentiating medium.

entiation has been demonstrated (Cosgrove and Cobbett, 1991), only morphologically differentiated and not non-differentiated N1E-115 cells have higher V_m and excitable membranes (Tuttle and Richelson, 1975; Moolenaar and Spector, 1977; Quandt et al., 1984), suggesting that morphological differentiation is a prerequisite for electrophysiological differentiation. The correlation between number of neurites and initial cell concentration shown in Fig. 8 supports the suggestion that morphological differentiation is a prerequisite for electrophysiological differentiation. This correlation between neurite development and initial cell concentration is also consistent with our current understanding of *in vivo* neuronal circuitry development. Nerve cells *in vivo* are wired to other nerve cells over distances that are regularly more than a thousand times larger than their cell bodies. One of the first steps in the formation of specific neuronal connections is the projection of axons to their target through diverse and changing environments. The selection of pathways by neuronal growth cones occurs with a high degree of precision and appears to be under control of locally acting guidance cues that direct growth cones to a succession of intermediate targets (Placzek et al., 1990). Molecular cloning of membrane-associated guidance proteins that also exist in soluble form has been successfully accomplished (Kennedy et al., 1994). Other factors, like nerve growth factors, have been implicated in axon guidance *in vitro* (Gundersen and Barrett, 1979), but related functions *in vivo* have remained obscure (Lumsden and Davies, 1983). It is evident that as neuronal tissue extends axons, the resulting outgrowth patterns must depend on whether factors in the medium are present as a homogeneous distribution or as a concentration gradient. It is conceivable that in tissue culture the concentrations of such factors depend

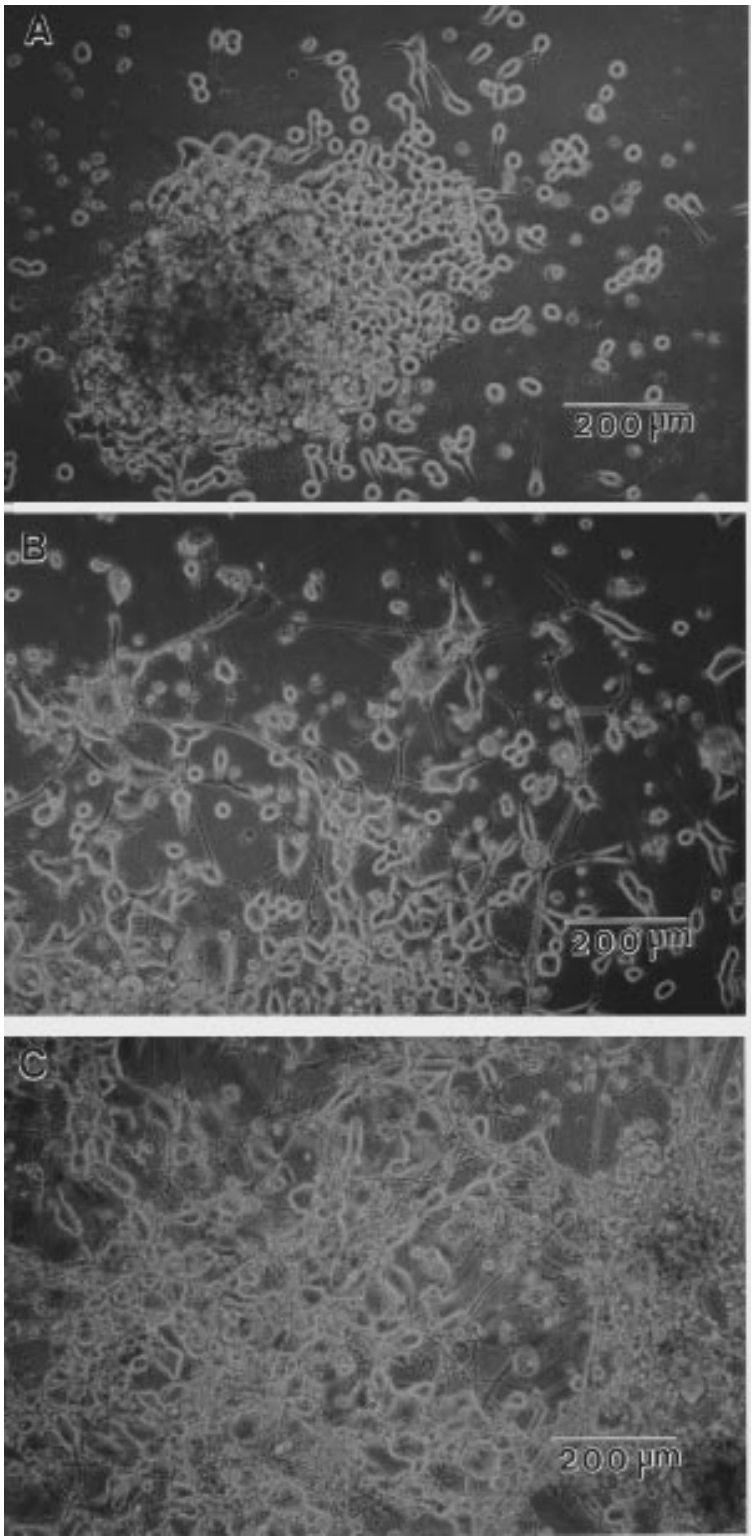

Figure 8. Representative N1E-115 phase contrast micrographs after 15 days of incubation with the differentiating medium. Cells were plated at: (A) 2,000; (B) 8,000; and (C) 80,000 cells per cm^2.

on cell densities, and therefore low initial cell concentration should result in less neurite formation and consequently delayed electrophysiological differentiation.

Implications for in vitro identification of neurotoxic potential

Risk assessment is typically viewed as an empirical process to determine the probability that an adverse health effect will be associated with exposure to a chemical. The NRC (1983) divided the risk assessment process into four major steps: (1) hazard identification, (2) dose-response assessment, (3) exposure assessment, and (4) risk characterization. With regard to neurotoxicology, hazard identification is the process of determining whether or not exposure to a chemical produces an adverse effect and whether that effect can be defined as neurotoxicity (Tilson, 1995). Neurotoxic effects can be defined as adverse effects on neurobehavior, neurophysiological, or neurochemical functioning and/or structural integrity of the nervous system (Tilson, 1990). Based on the premise that interference of toxic agent with the integrity of excitable cell membranes usually causes serious impairment of the function of important organ systems and that such effects on the nervous system inevitably lead to alterations in impulse propagation, the results presented above can be utilized in neurotoxic safety/hazard evaluation, and/or risk assessment in several ways. For example, with the V_m-development profile presented in Fig. 5 as the control, both compounds with and without known *in vivo* neurotoxic effect can be evaluated with respect to interference with 'normal' $V_m$development. Correct assignment of compounds with known neurotoxic effect would attest to the suitability of the test for the unknown. Alternatively, differentiation-stage dependence of neurotoxic expression can be established by using cells at different electrophysiological differentiation stages (Kisaalita and Bowen, 1996).

Conclusions

This investigation showed that the relative distribution of differentiating/differentiated murine neuroblastoma cells (N1E-115) between low and high FALS as determined by flow cytometry has the potential to act as a culture differentiation state index covering periods before and after terminal differentiation. This finding should be extendable to other excitable cells of nervous system origin. Using a large viable cell population (50,000), this investigation has further demonstrated that initial cell concentration influences the electrophysiological differentiation (characterized by resting membrane potential development) time-profile of N1E-115 cells. At low initial cell densities ($< 2 \times 10^4$ cell/cm^2), V_m development was slower and at higher initial cell densities full V_m development was achieved by day 12 under differentiation culture conditions (low serum– 0.5% FBS). Exact differentiation time-profiles information is essential in studies employing neuroblastoma cells as engineered tissue or *in vitro* models of some aspects of nervous system development, such as uses for *in vitro* safety/hazard evaluation and/or risk assessment of therapeutical and industrial chemicals under development.

Acknowledgments

The authors thank Joby Miller and Manju Amin for their technical support. This research was supported through a University of Georgia Faculty Research Grant to WSK and State and Hatch funds appropriated to the University of Georgia, College of Agricultural and Environmental Sciences Experiment Stations. Mention of brand names is for information only and does not imply endorsement.

References

Amano T, Richelson E and Nirenberg M (1972) Neurotransmitter synthesis by neuroblastoma clones. Proc. Natl. Acad. Sci. 69: 258–263.

Augusti-Tocco G and Sato G (1969) Establishment of functional clonal lines of neuroblastoma clones. Proc Natl. Acad. Sci. 64: 311–315.

Bashford CL, Alder GM, Gray MA, Micklem KJ, Taylor CC, Turek T and Pasternak CA (1985) Oxonol dyes as monitors of membrane potential of animal cells in monolayer culture and in suspension. J. Cell Physiol. 123: 326–336,

Baumgold J and Spector I (1987) Development of sodium channel protein during chemically induced differentiation of neuroblastoma cells. J. Neurochem. 48: 1264–1269.

Bräuner T, Hülser TF and Straser RJ (1984) Comparative measurements of membrane potentials with microelectrodes and voltage-sensitive dyes. Biochim. Biophys. Acta 771: 208–216.

Chalazonitis A and Green LA (1974) Enhancement in excitability properties of mouse neuroblastoma cells in the presence of dibutyl cyclic AMP. Brain Res. 72: 340–345.

Cosgrove C and Cobbett P (1991) Induction of temporally dissociated morphological and physiological differentiation of N1E-115 cells. Brain Res. Bull. 27: 53–58.

Couly GF, Coltey PM and Le Douarin NM (1993) The triple origin of skull in higher vertebrates – A study in quail-chick chimeras.

Development. 117: 409–429.
Dwyer TM and Cuchens M (1987) Membrane potential measurements by flow cytometry. J. Electrophysiol. Tech. 14: 43–57.
EPA (1991) EPA's research strategies for the 1990s. Vet. Human Toxicol. 33: 69–70.
Fishman MC and Spector I (1981) Potassium currents suppression by quinidine reveals additional calcium currents in neuroblastoma cells. Proc. Natl. Acad. Sci. 78: 5245–5249.
Gilbert JA, Knodel EL, Stenstrom SD and Richelson E (1982) Function and regulation of methionine^5-encephalon and its receptors in murine neuroblastoma cells. J. Biol. Chem. 257: 1274–1281.
Givan AL (1992) Flow Cytometry: First Principles, pp. 90–91, Wiley, New York.
Gunderson RW and Berrett JN (1979) Neuronal chemotaxis: chick dorsal-root axons turn toward high concentrations of nerve growth factor. Science 206: 1079–1080.
Hogg RV and Craig AT (1995) Introduction to Mathematical Statistics, pp. 521–526, Prentice-Hall, New Jersey.
Ishikawa S (1977) Differentiation of human neuroblastoma cells *in vitro* – morphological changes induced by dibutyryl cyclic AMP. Acta Path. Jap. 27: 697–711.
Kato E and Narahashi T (1982) Characteristics of the electrical response to dopamine in neuroblastoma cells. J. Physiol. 333: 213–226.
Kennedy TE, Serafini T, de la Torre JR and Tessier-Lavigne M (1994) Netrins are diffusible chemotropic factors for commissural axons in the embryonic spinal cord. Cell 78: 425–435.
Kimhi Y, Palfrey C, Spector I, Barak Y and Littauer UZ (1976) Maturation of neuroblastoma cells in the presence of dimethylsulfoxide. Proc. Nat. Acad. Sci. 73: 462–466.
Kisaalita WS and Bowen JM (1996) Effect of culture age on the susceptibility of differentiating neuroblastoma cells to retinois cytotoxicity. Biotechnol. Bioeng. 50: 580–586.
Kisaalita WS, Lund RB and Evans MD (1996) Size changes in differentiating neuroblastoma cells. In Vitro accepted.
Kohen E and Hirschberg JA (1989) Cell Structure and Function by Microspectrofluorometry. Academic Press, New York.
Krieger C, Paul E and Kim, SU (1991) Development of resting membrane potentials of embryonic murine spinal cord cells evaluated by flow cytometry analysis. Dev. Neurosci. 13: 11–19.
Lumsden A and Davies A (1983) Earliest sensory nerve fibers are guided to peripheral targets by attractants other than nerve growth factor. Nature 306: 786–788.
Miyake M and Kurihara K (1983) Resting potential of the mouse neuroblastoma cells I: The presence of K^+ channels activated at high K^+ concentration but closed at low K^+ concentration including the physiological concentration. Biochim. Biophys. Acta 762: 248–255.
Moolenaar WH and Spector I (1977) Membrane currents examined under voltage clamp in cultured neuroblastoma cells. Science 196: 331–333.
Nummery CL, Van Den Brink CE, Van Der Saag PT and De Laat SW (1984) A short-term screening test for teratogens using differentiating neuroblastoma cells. Teratology 29: 271–279.
Nelson PG, Ruffner BW and Nirenberg MW (1969) Neuronal tumor cells with excitable membranes grown *in vitro.* Proc. Natl. Acad. Sci. 64: 1004–1010.
NRC (1983) Risk Assessment in the Federal Government: Managing the Process. National Academy Press, Washington D.C.
Orkland RK (1977) Glial cells. In: Kandel ER (ed) Cellular Biology of Neurons, pp. 855–875, American Physiological Society, Bethesda, MD.
Peacock JH, Mina J, Nelson PG (1972) The use of aminopterin in selecting electrically active neuroblastoma cells. Exp. Cell Res. 73: 367–377.
Plazek M, Tessier-Lavigne M, Yamada T, Dood J and Jessell TM (1990) Guidance of developing axons by diffusible chemoattractants. Cold Springs Harbor Symp. Quant. Biol. 55: 279–289.
Quandt FN and Narahashi T (1994) Isolation and kinetic analysis of inward currents in neuroblastoma cells. Neuroscience 13: 249–262.
Ramsden JJ, Li S-Y, Prenosil JE and Heinzle E (1993) Kinetics of adhesion and spreading of animal cells. Biotechnol. Bioeng. 43: 939–945.
Rouget P, Le Bert M, Borde and Evrard C (1992) Generation of neural cell lines by transfer of viral oncogenes. In: Woods JN (ed) Neuronal Cell Lines: A Practical Approach, pp. 27–54, Oxford University Press, Oxford.
Santone KS, Oakes GS, Taylor SR and Powis G (1986) Anthracycline-induced inhibition of calcium action potential in differentiated murine neuroblastoma cells. Cancer Res. 46: 2659–2664.
Seeds NW, Gilman AG, Amano T and Nirenberg MW (1970) Regulation of axon formation by clonal lines. Proc. Nat. Acad. Sci. 66: 160–167.
Spector I (1981) Electrophysiology of clonal nerve cell lines. In: Nelson PG and Liebermann M (ed) Excitable Cells in Tissue Culture, pp. 257–277, Plenum, New York.
Tilson HA (1995) Risk assessment for neurotoxicity: An introductory overview. In: Chang LW and Slikker W (eds) Neurotoxicology: Approaches and Methods, pp 767–770, Academic Press, New York.
Tosney KW (1982) The segregation and early migration of cranial neural crest cells in avian embryo. Dev. Biol. 89: 13–24.
Tuttle JB and Richelson E (1975) Ionic excitation of a clone of mouse neuroblastoma. Brain Res. 84: 128–135.
Veronesi B (1992) The use of cell culture for evaluating neurotoxicity. In: Tilson H and Mitchel C (eds) Neurotoxicology, pp. 21–49, Raven Press, New York.
Walum E, Ekblad-Sekund G, Nyberg E and Gustafsson L (1987) Cultured neuroblastoma cells as neurotoxicological models: Acrylamide induced neurite disintegration. In: Shaler A and Goldber AM (eds) Model Systems in Neurotoxicology: Alternative Approaches to Animal Testing, pp. 121–136, Alan Liss, New York.
Walum E, Nordin M, Beckman M and Odland L (1993) Cellular methods for identification of neurotoxic chemicals and estimation of neurotoxicological risk. Toxic. *in Vitro.* 7: 321–326.
Williams SP, Davenport-Jones J, Egan C, O'Hare S, Cookson M, McClean R and Garle MJ, Pentreath V and Atterwill CH (1994) Phase 1 of an *in vitro* neurotoxicological pre-validation trial. Toxic. *in Vitro.* 8: 799–802.
Wilson HA and Chused TM (1985) Lymphocyte membrane potentials and Ca^{2+}-sensitive potassium channels described by oxonol dye fluorescence measurements. J. Cell. Physiol. 125: 72–81.
Zwart R, Abraham D, Oortgiessen M, and Vijverberg HPM (1994) $\alpha 4\beta 2$ subunits combination specific pharmacology of neuronal nicotinic acetylcholine receptors in N1E-115 neuroblastoma cells. Brain Res. 654: 312–318.

Address for correspondence: Dr. W.S. Kisaalita, University of Georgia, Biological and Agricultural Engineering Department, Driftmier Engineering Center, Athens, GA 30602, USA